

NATO UNCLASSIFIED



NATO Undersea Research Centre
Centre de Recherche Sous-Marine de l'OTAN



NURC Technical Report

SR-443

Infrared detection of marine mammals

Alberto Baldacci, Michael Carron and Nicola Portunato

December 2005

This document is for distribution only to NATO, Government Agencies of NATO member nations and their contractors. Requests for secondary distribution shall be made to the NATO Undersea Research Centre (NURC).

Releasable for Internet Transmission

Official Information

NATO UNCLASSIFIED

No Public Release

NATO Undersea Research Centre (NURC)

NURC conducts world class maritime research in support of NATO's operational and transformational requirements. Reporting to the Supreme Allied Commander Transformation, the Centre maintains extensive partnering to expand its research output, promote maritime innovation and foster more rapid implementation of research products.

The Scientific Programme of Work (SPOW) is the core of the Centre's activities and is organized into four Research Thrust Areas:

- Expeditionary Mine Countermeasures (MCM) and Port Protection (EMP)
- Reconnaissance, Surveillance and Undersea Networks (RSN)
- Expeditionary Operations Support (EOS)
- Command and Operational Support (COS)

NURC also provides services to other sponsors through the Supplementary Work Program (SWP). These activities are undertaken to accelerate implementation of new military capabilities for NATO and the Nations, to provide assistance to the Nations, and to ensure that the Centre's maritime capabilities are sustained in a fully productive and economic manner. Examples of supplementary work include ship chartering, military experimentation, collaborative work with or services to Nations and industry.

NURC's plans and operations are extensively and regularly reviewed by outside bodies including peer review of the research, independent national expert oversight, review of proposed deliverables by military user authorities, and independent business process certification. The Scientific Committee of National Representatives, membership of which is open to all NATO nations, provides scientific guidance to the Centre and the Supreme Allied Commander Transformation.



Copyright © NATO Undersea Research Centre 2005. NATO member nations have unlimited rights to use, modify, reproduce, release, perform, display or disclose these materials, and to authorize others to do so for government purposes. Any reproductions marked with this legend must also reproduce these markings. All other rights and uses except those permitted by copyright law are reserved by the copyright owner.

Single copies of this publication or of a part of it may be made for individual use only. The approval of the NURC Information Services Branch is required for more than one copy to be made or an extract included in another publication. Requests to do so should be sent to the address on the back cover.

Infrared Detection of Marine Mammals

Alberto Baldacci, Michael Carron
and Nicola Portunato

The content of this document pertains to work performed under Project 4F1 of the NATO Undersea Research Centre Programme of Work. The document has been approved for public release by the Director, NATO Undersea Research Centre, La Spezia, Italy.

Steven E. Ramberg
Director

Intentionally blank page

Infrared Detection of Marine Mammals

Alberto Baldacci, Michael Carron, Nicola Portunato

Executive Summary: The Marine Mammal Risk Mitigation program at the NATO Undersea Research Centre (NURC) is responsible for developing and testing on-scene marine mammal observation devices. Visual monitoring, supplemented by acoustic monitoring, is the primary method used in NURC research experiments to perform on-scene risk assessment and mitigation. However, visual monitoring cannot be employed at night, in inclement weather or in high waves (greater than sea-state 3). Since marine mammals do not vocalize continuously or have vocalizations which are difficult to identify at long ranges, additional supplementary methods, including the use of radar and infrared (IR) devices, are also being assessed. During the summer of 2003 a military IR device was tested during the Sirena 03 sea trial onboard the NATO Research Vessel (NRV) *Alliance* during the *Mar Ligure Joint Experiment 2003* (MLJX'03). This report documents the results of this preliminary experiment.

Intentionally blank page

Infrared Detection of Marine Mammals

Alberto Baldacci, Michael Carron, Nicola Portunato

Abstract:

An infrared (IR) binocular, designed for in-the-field military applications, was tested using in situ marine mammals during the Mar Ligure Joint Experiment 2003 (MLJX'03) that took place in August-September 2003 onboard the NRV *Alliance*. The test investigated the potential of IR technology for marine mammal detection, in both day time and night time conditions. The effectiveness of this IR system in detecting marine mammals was strongly affected by weather conditions, ranging from excellent performance during clear and low sea-state conditions to poor performance during hazy conditions or higher sea-states. The IR system was tested during both day and night.

Keywords: marine mammal risk mitigation, cetacean, whale, infrared, IR, detection, blow temperature, surface temperature.

Contents

1. Introduction	1
2. Principles of IR Systems	3
2.1 <i>Classification of IR systems</i>	4
3. The use of IR technology for marine biology observation and study.....	6
4. Experimental Setup	9
4.1 <i>Overview</i>	9
4.2 <i>IR Binoculars</i>	9
4.3 <i>Auxiliary Systems</i>	10
4.4 <i>Auxiliary Data</i>	10
5. IR Recordings and Data Analysis.....	12
5.1 <i>Overview</i>	12
5.2 <i>Sensor Calibration and Offline Correction</i>	15
5.3 <i>Comparison Between Visual Sightings and IR Sightings</i>	16
6. Lessons Learned and Future Work.....	25
7. Conclusions	27
References	28
Acknowledgements	29
Annex A – Principles of Thermography	30

The Marine Mammal Risk Mitigation (MMRM) program at the NATO Undersea Research Centre (NURC) is investigating, among others, non-traditional observation methods of marine mammals, especially for use during night-time sonar experiments. In the past, night vision visual amplifiers were tested, but were abandoned because results were limited [1]. As an alternative, the Centre is looking into the potential of Infrared (IR) technology for night visual watch.

IR systems are capable of detecting differences in temperature from radiated thermal energy from living bodies or from reflected and scattered thermal energy. IR systems are much like video cameras equipped with a sensor that is sensitive to the IR portion of the electro – magnetic spectrum. Since water is opaque to IR radiation and a layer of few microns of water is enough to completely attenuate it, marine mammals can be detected only when they come to the surface. Possible detection spots are the body, the fins, the blow and the blow hole.

Marine Mammal detection by means of IR Video may be possible in daytime conditions, as well. IR sensitivity to reflected and refracted solar radiation may in some cases produce even better results than detection through classic video systems like regular binoculars. But the absence of solar radiation (during night time conditions) presents a particular challenge for IR Video: because cetaceans have extremely effective thermal insulation, there is only a small temperature difference between the animal's skin and the surrounding water. Even if the animals come to the surface, they are still covered by a thin layer of water, often masking the temperature of the body [7].

The *Mar Ligure Joint Experiment 2003 (MLJX'03)* took place in August-September 2003, with the participation of the two NATO vessels NRV *Alliance* and CRV *Leonardo*, the Italian Hydrographic Office ship *Ammiraglio Magnaghi* and the Italian government Research Vessel *Urania*. During Phase 1 of the experiment, aimed at monitoring the presence of marine mammals in a region west of Sardinia and Corsica, IR binoculars were tested (in both day-time and night-time conditions) for nine days on board of NRV *Alliance*. The track of the vessel during this phase is shown in Figure 1. During the experiment, many marine mammals were encountered, so it was possible to compare regular visual sightings with IR sightings. Some IR video sequences were recorded and significant frames are shown in this work.

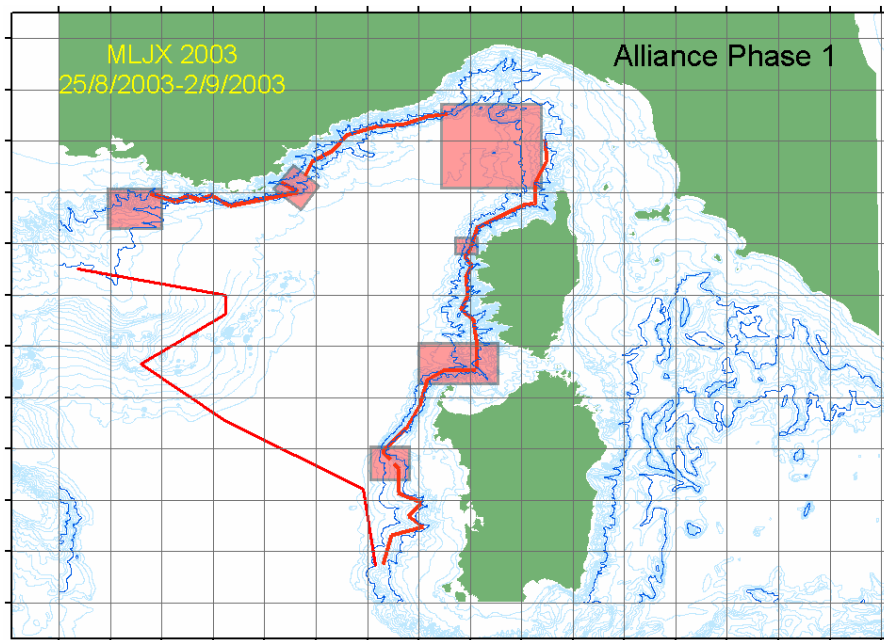


Figure 1 NRV Alliance planned track for Sirena'03 – Phase 1.

This report is organized as follows: The principles and classification of IR systems are discussed in Section 2. Some applications of IR technology with respect to marine mammals are listed in Section 3. Section 4 describes the experimental setup, instruments, methodology. Examples of IR recordings are shown in Section 5. The conclusions are explained in Section 7.

2

Principles of IR Systems

A thermal imager is an IR analogue of a TV camera. The purpose of a thermal imager is to detect the natural radiation emitted by all material bodies. This radiation is described by various forms of the Plank radiation law (refer to Annex A, for details).

IR energy is absorbed by various chemical compounds found in the atmosphere. However, there are several "windows" in the spectrum in which absorption is minimized and radiation detectable. Figure 2 demonstrates why the most common bands of interest are the 3 to 5 and 8 to 14 μm regions. These two bands have the least atmospheric absorption under standard atmospheric conditions. A system operating anywhere in the 8 to 14 μm region is usually referred to as a Long Wave IR (LWIR) system; and one operating anywhere in the 3 to 5 μm region as a Medium Wavelength IR (MWIR). The presence of high humidity, clouds, fog or smoke can dramatically increase IR absorption.

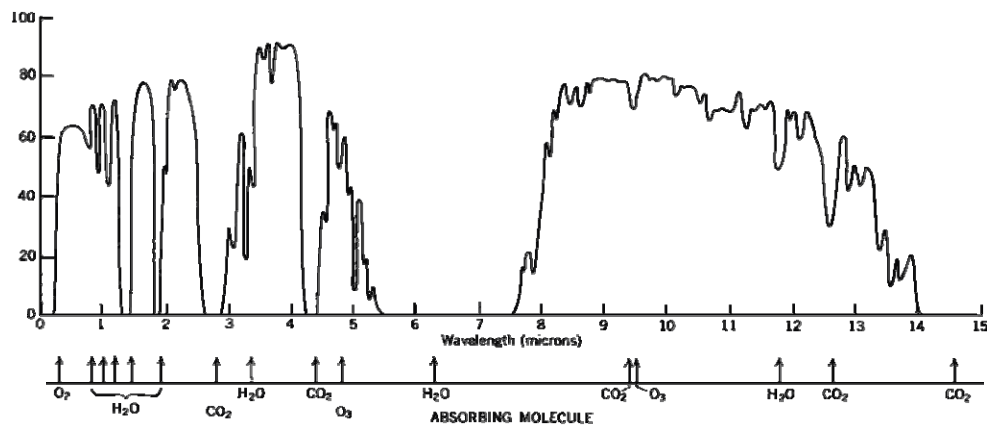


Figure 2 Spectral atmospheric transmissivity [6].

It is important to note that thermal imager operation is different than the other types of night vision devices that operate in the near darkness by amplifying existing visible (or near--visible) external radiation (from moonlight, starlight, sky-glow, etc). These systems are quite common and operate very well if there is sufficient external illumination. They cease to operate altogether in absolute darkness or in deep shadows. Also, they do not *see* as well as thermal imagers through smoke, dust, haze, etc. In contrast, the thermal imager is a system that provides a visible rendition of the invisible IR radiation scene.

In the last few years, thermal imaging sensors with high radiometric sensitivity and high geometric resolution have been developed. Such technological advancements have allowed for passive detection, classification and identification of both maritime and terrestrial targets in an environment with many potential false targets. Advantages of using the IR portion of the spectrum include the high geometric resolution it provides, the availability of small and lightweight IR equipment; and, above all, its day and night operational capability [3][4].

Of course, IR systems also have limitations. As previously discussed, one of the main problems is related to the atmospheric attenuation of IR energy. IR sensors may also be affected by sun-glint— reflection of solar radiation toward the optics, causing a particularly negative degradation in the MW band where the solar spectral radiance is maximum.

2.1 *Classification of IR systems*

IR systems can be divided into two categories: calibrated systems and thermal imagers [5].

Calibrated IR systems measure the temperature of a body by detecting the amount of energy radiated by the body and converting it to surface temperature given some parameters like the emissivity of the body (see Annex A), the estimated atmospheric attenuation and atmospheric irradiance. Calibrated IR systems are mainly used in thermography for maintenance of electric systems; usually having high thermal sensitivity, but low geometric resolution.

Thermal imagers, the second category of IR systems, are much like TV cameras, except that they operate in the IR region of the electromagnetic spectrum. A lens focuses scene information onto a detector, which converts the perceived IR energy to an electrical signal displayed on a monitor or sent to a processing unit. Thermal imagers can detect temperature differences, but cannot calculate the actual temperature of the emitting body. Usually thermal imagers are characterized by both high thermal sensitivity and high geometrical resolution.

Thermal imagers are mainly used for detection and recognition purposes. In this paper we will focus on Forward Looking IR (FLIR) sensors. The purpose of a FLIR is to provide a visible representation of the invisible-to-humans IR radiation scene, based on the natural radiation emitted by material bodies. FLIRs can be characterized in terms of Field of View (FOV), frame rate and number of pixels:

- ❑ Field of View: the standard FLIR has a relatively small FOV. Wide-FOV FLIRs are not uncommon, but usually have low-resolution. A typical FOV is 8° (horizontal) by 6° (vertical).
- ❑ Frame rate: the typical FLIR is designed to produce real-time display for human observers; thus, it has high frame rates to avoid image flicker. 25Hz

(CCIR standard, diffused in Europe) and 30Hz (RS-170 standard, diffused in the US) are most often used.

- Number of pixels: the small FOW of FLIRs results in relative small number of pixels compared to, for instance, IR Search and Track (IRST) systems; image dimensions rarely exceed 1024×1024 pixels; usually dimensions of 640×480 or smaller are adopted.

Beyond the two primary categories, IR sensors may be further classified by the way a frame of video is generated and by a detector device. FLIR thermal imagers can be divided into two main classes: ones with staring or scanning sensors [5]. Thanks to recent improvements in charged-coupled device (CCD) technology, most of FLIRs are equipped with staring sensors, which utilize a two-dimensional array of detectors to sample the scene at a given focal plane. Each detector in the array corresponds to a pixel in the image. Modern staring systems are based on Focal Plane Array (FPA) technology, where the detector matrix is a bulk solid-state device in which sampling and signal pre-processing take place in the same integrated circuit. Staring-sensor focal planes collect optical radiation and direct the radiation onto a photon-detecting surface to convert the image to a charge-carrier pattern.

Historically, staring sensors cover the shorter wavelengths (MWIR); scanning sensors, the longer wavelengths (LWIR). The evolution of this division of spectral coverage has been driven by physical principles and engineering restrictions [6].

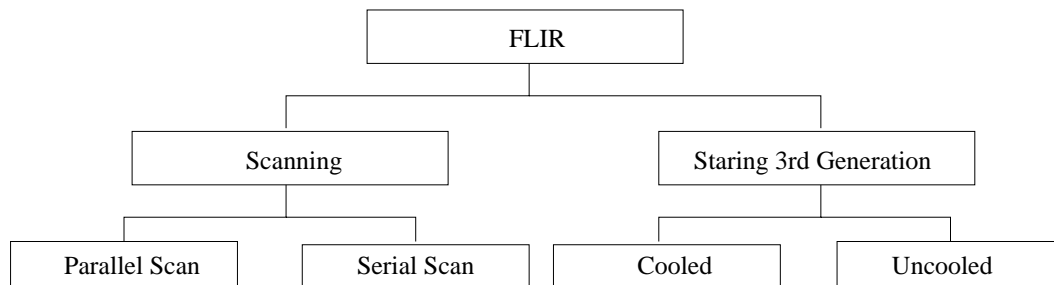


Figure 3 Classification of IR sensors.

3

The use of IR technology for marine biology observation and study

The use of IR systems for marine mammal observation and study is limited by physics to surfacing animals only. Water is non transparent to thermal radiation, and an IR system cannot see anything below (even few microns) the sea surface. Even surfacing animals are covered by a thin layer of water, which partially or completely masks the body temperature. Consequently, it's more correct to speak of an animal's surface temperature rather than skin temperature [7].

Despite the masking and efficient thermal insulation of marine mammals, [8], a temperature gradient is present, if extremely low. Also, state of the art thermal imagers are extremely sensitive, capable of discriminating temperature differences of one tenth of degree, making this technology potentially good enough for marine mammal detection applications [6].

A recent experiment, aimed at studying the thermoregulation at depth of bottlenose dolphins, made use of IR calibrated cameras and thermistors implanted on the animals [9]. The results of this study showed that the thick insulating blubber layers that encase the body of cetaceans mask their own thermal radiation. Nonetheless there are some poorly insulated peripheral areas on cetaceans' bodies: these thermal windows emit excess heat from the body during periods of high activity or when the ambient water is warm. Specifically, on whales and dolphins these peripheral areas are their flukes, dorsal fins and pectoral fins [10]. Figure 4 is an example of a thermograph of a fluke, created with a calibrated IR sensor [9].

During this experiment, surface skin temperature of the dolphins remained within 1°C of ambient water temperature during resting and diving (see Figure 5). For dolphins resting on the surface, no significant temperature difference was found for five different anatomical sites. Measurement sites included both insulated central areas and peripheral thermal windows. Mean skin temperatures of the peripheral sites were measured to be 0.4 – 0.6°C lower for resting dolphins than diving dolphins.

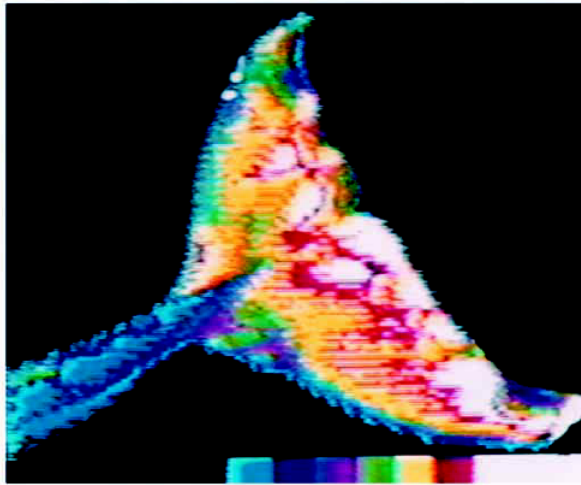


Figure 4 IR thermograph of the fluke of a bottlenose dolphin. Warm areas (denoted by white and red) correspond to large blood vessels that traverse the width of the underside of the fluke. Note the comparatively cool peduncle area shown in blue. The colour bar at the bottom denotes 0.1 °C differences in surface temperature per gradation. [9]

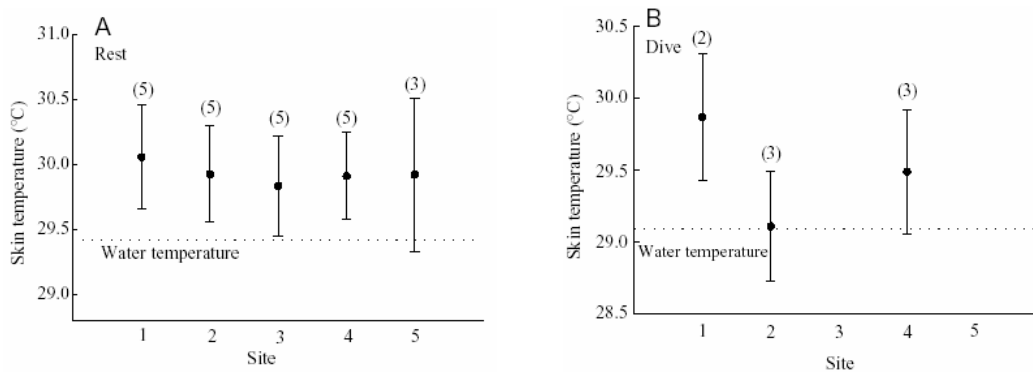


Figure 5 Skin temperature for different anatomical sites of resting (A) and diving (B) bottlenose dolphins. Mean values ± 1 S.E.M. are presented. Numbers in parentheses represent the number of measurements in each data set for up to five dolphins. Anatomical sites are as follows: 1, dorsal fin; 2, mid flank; 3, mid peduncle; 4, underside of the fluke; and 5, underside of the pectoral fin. The horizontal dashed lines represent the water temperature at the measurement location (i.e. holding pen temperature for resting studies and ocean temperature at the dive site for the diving measurements) [9].

Potential targets of thermal detection also include the blow, the blowhole and areas of water perturbation due to the animal's movement, which may mix water of different temperatures. Finally, thermal imagers are sensitive to solar energy scattered and

reflected off disturbed water and the animal itself, providing more detection opportunities, particularly in the MWIR band, where the solar irradiance is at its maximum.

These detection possibilities were investigated during another experiment, focused on testing new detection techniques and obtaining information on whale surface temperature in northern seas [7]. An Agema Thermovision 880 calibrated camera, operating in the 8 to 12 μ m band, was used to detect thermal IR radiation from whales. The camera used scanning technology and had a nominal sensitivity of 0.07°C at 30°C object temperature. During the experiment, minke, humpback, fin, blue and sperm whales were observed; all observations were made during daylight. The results showed that the observed radiation temperature was strongly dependent on sea conditions, signal angle and atmospheric interference. Masking and good thermal insulation also made observations difficult. When a surfacing minke whale was covered by a thin film of water, its thermal radiation was completely masked: the temperature difference between the animal and the surrounding water was usually less than 0.1°. For the other observed species, the difference was less than 1.0°. As expected, detection performance based on body temperature was extremely poor (with detection ranges as small as 150m maximum distance), even in favourable weather and sea conditions. Blue whales could be detected at a distance of about 1Km because of their blows; the maximum temperature difference between seawater and blow was 4.0°C, while the maximum difference for the blowhole was 4.1°C [7].

No other related experiments have been reported in the open scientific literature to the best of our knowledge. For detection purposes, the performance summarized above may seem to suggest that the use of IR systems for observation is useless; nonetheless, this experiment took place in 1989, and IR technology has improved a lot during recent years, especially thanks to the use of focal plane arrays with high thermal sensitivity and geometric resolution. Furthermore, a calibrated camera was used, which is suitable for experiments where the actual temperature of the observed object is needed, while is not the best choice for detection purposes. For this application a forward looking IR (FLIR) system is more effective, thanks to its higher thermal sensitivity and geometric resolution. The IR system used in our experiment is a third generation FLIR (see section 4.2), so we expected to obtain better performance.

4

Experimental Setup

4.1 Overview

IR binoculars and a digital video camera (Figure 6) were the equipment tested. These two systems were mounted on a tripod and had approximately parallel optical axes. The field of view was set, when possible, to be also the same, to allow for comparison between what could be seen in the visible and what was measured in the IR. The tripod was installed on the flying bridge of the NRV *Alliance*, 14 meters above the sea surface. The geometric horizon (i.e. the horizon due to the curvature of the Earth) was about 13Km (7.4nmi).

The analog video output was digitalized for post-processing. Some other modules were necessary to complete the acquisition and analysis system. These systems are shortly described in the following sections.

4.2 IR Binoculars

The IR binoculars used in this experiment were SAGEM MATIS (Medium wavelength Advanced Thermal Imaging System) Handheld thermal imager [11][12][13]. It is a one-piece, fully autonomous camera that integrates bi-ocular display, controls and a battery pack. Its sensor employs staring technology: the detector is an Indium Antimonide (InSb) focal plane array (FPA) matrix of 384×256 elements. The operating band is 3-5 μ m with a sensitivity ≤ 35 mK at ambient temperature. The integration time may be either automatically adjusted to suit the scene or modified by hand. The working temperature is 77K: the detector is cooled down to this temperature by a cryogenic system based on the Stirling cycle; it takes about 6 minutes to cool.

The system has two optical fields of view: 9° (horizontal) by 6° (vertical) in wide field of view (WFOV) and 3°×2° in narrow field of view (NFOV). In addition, 2× digital zoom is available. The aperture is f/4. The focus may be manually adjusted.

Commands include: gain-contrast adjustment and Automatic Gain Control (AGC); level/brightness adjustment; detector calibration; detector integration time change.

The MATIS Handheld has a single external connector ensuring CCIR video output (analog), external power supply input and RS422 data communication. Only the video output capability was used during the experiment to record the video sequences of interest.

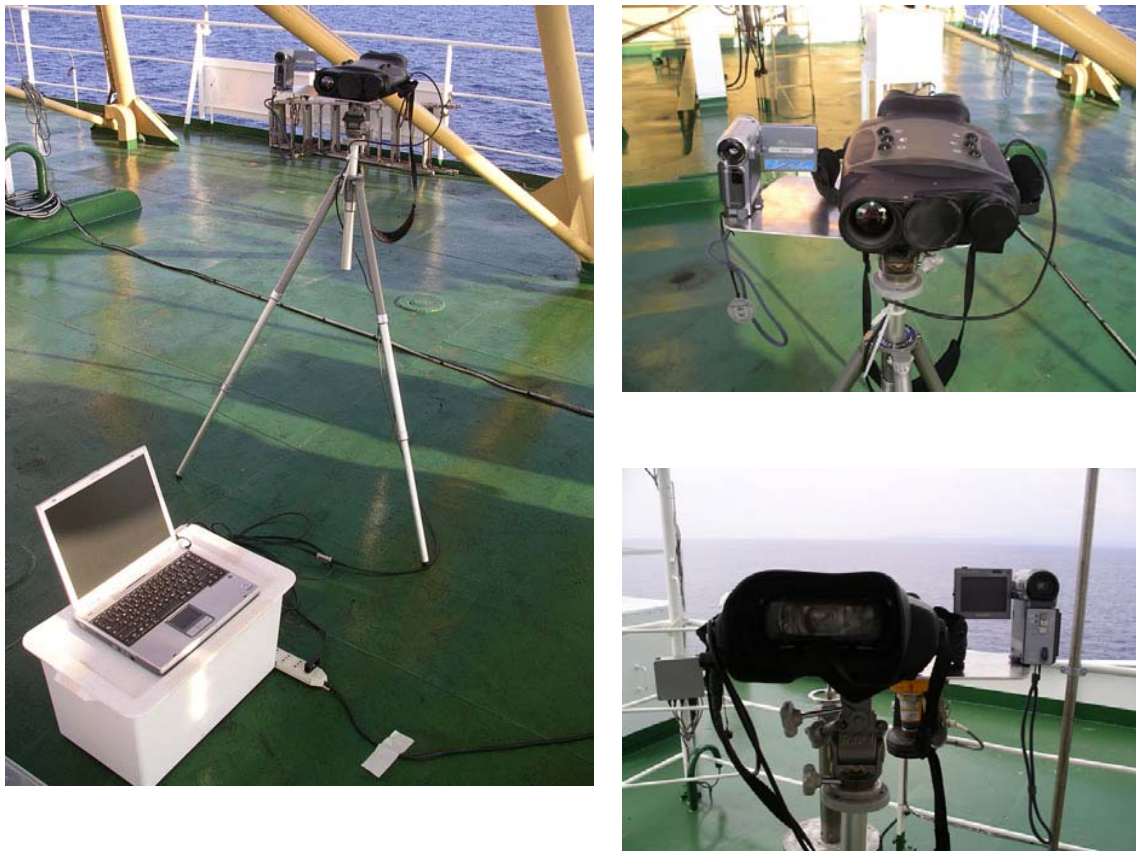


Figure 6 Instruments used for the experiment: tripod with IR binocular and digital video camera, and controlling unit consisting in a laptop and in an analog to digital converter (not shown). On the right, front and rear view of the IR binocular and of the digital video camera.



Figure 7 Particular of the tripod showing the bearing scale (left) used to point the devices to the direction detected through the long range binoculars (right).

4.3 Auxiliary Systems

- ❑ Digital Video Camera. For comparison with IR sequences, a standard digital video camera was used in daylight conditions to collect video sequences. The camera was a SONY MicroMV video camera, recording video sequences of 720 X 576 pixels, 25 frames per seconds. The video streams were internally converted to Digital Video file format, based on MPEG2 video compression (DVD video quality). Date and time are stored together with the video signal, so that recordings can be synchronized with IR data.
- ❑ Analog to Digital Converter. Since the thermal imager provides analog video output only, an A/D converter was used to digitalize the output of the binoculars and store it to disk. The acquisition box was a Pinnacle Studio Movie Box DV, capable of a high data rate thanks to the firewire (IEEE1394) link to the controlling laptop. Video streams were usually acquired with the highest possible data rate, in order to have the lowest compression rate and the best quality.
- ❑ Laptop. A laptop served as a convenient portable controlling unit for the analog to digital converter on the flying bridge. It was also used to analyse recorded data in the *Alliance*'s main laboratory.
- ❑ Tripod. To guarantee more stable images and that the thermal imager and the video camera had the same optical axis, the two optical systems were mounted on a common mechanical interface installed on top of a tripod. The tripod had a bearing reference with 5 deg ticks (Figure 7), which were used during the experiment to help pinpoint the animals through the long range binoculars (25 ×10, also known as “big eyes”).

4.4 Auxiliary Data

- ❑ Meteorological data. Atmospheric attenuation of IR radiation is mainly due to humidity. Further, in daytime operations, the reflection of solar radiation over the sea surface and cloud cover is responsible for sea clutter. For this purpose, the meteorological data acquired by the meteorological station of the *Alliance* have been recorded for further investigation.
- ❑ Sighting reports. Every time there was a visual sighting, date and time of the sighting, distance of the animal, aspect relevant to the boat, behaviour, first cue and many other was recorded. These data are fundamental to understand the IR system performance.

5

IR Recordings and Data Analysis

5.1 Overview

During Sirena'03 Phase 1 Experiment the total observation time with the IR binoculars was about 13 hours over the first 3 days, plus about 10 hours over the first three nights. There were only short observation periods during the following days.

IR videos acquired by the analog to digital converter were saved as .AVI files with the characteristics shown in Table 1. A collection of IR videos in AVI format can be found in [14].

Table 1 AVI file characteristics

Frame rate	25 frames per second
Frame width	720 columns
Frame height	576 rows
Image type	True colour RGB
Video Compressor	Intel Indeo 5
Quality	100 (maximum quality)
Quantization	Unsigned integer, 1 byte per channel (256 levels, from 0 to 255)

Examples of AVI frames acquired during the day are shown in Figure 8 - Figure 10. The first three frames portray the same daytime scene taken with the three fields of view allowed by the instrument: wide field of view (camera mode: WFV, $9^{\circ} \times 6^{\circ}$), narrow field of view (camera mode: NFV, $3^{\circ} \times 2^{\circ}$) and $2 \times$ digital zoom or magnification (camera mode: MAG, $1.5^{\circ} \times 1^{\circ}$). The white box in the WFV image shows the portion of scene corresponding to the NFV. The white box in the NFV correspond the portion of scene corresponding to the MAG mode. Digital zoom simply magnifies the pixels of the central part of the original image by repeating them twice horizontally and vertically--no interpolation is used. The image appears blurred. Since the amount of information in MAG mode is the same as in NFV mode, the former mode was never used during the experiment. In all images, lighter pixels correspond to warmer areas, but it is not possible to infer the temperature of the corresponding radiating body. Nonetheless, it is clear that the land and the mountains on the background are warmer than the water. Further, the sea surface looks uniform, because the sea is calm (sea state 0.5-1, wind speed 1kt).

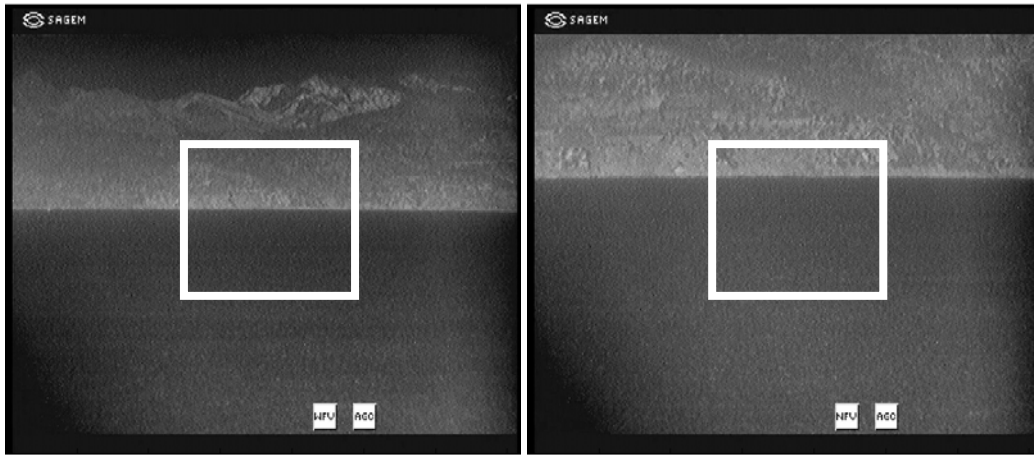


Figure 8 Examples of acquired frame. Left: wide field of view ($9^\circ \times 6^\circ$). Right: narrow field of view ($3^\circ \times 2^\circ$).

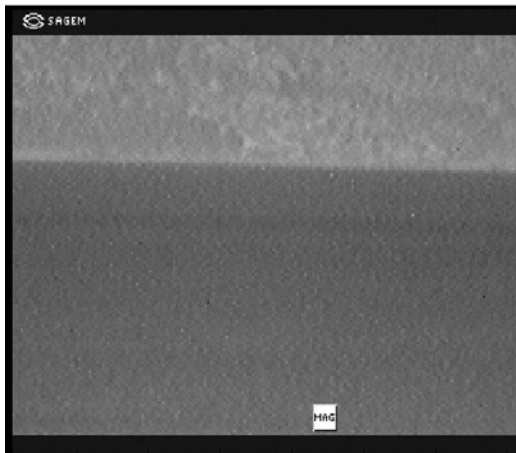


Figure 9 Example of acquired frame, 2x digital zoom ($1.5^\circ \times 1^\circ$)

When the sea state is higher (sea state 3 or more), significant sea clutter occurs (Figure 10, left).

One of the causes of IR sea clutter is solar reflection off of the sea surface: unsurprisingly, more clutter occurs when the sea surface is rough, each wave scattering the light. Observation is particularly difficult when breaking waves appear on the surface, or in the presence of white caps due to strong wind. Of course this type of sea clutter

occurs when there are strong light sources, especially the sun. This type of clutter is referred to specifically as *reflected clutter*.

Unfortunately, sea clutter may affect IR images in the total absence of light as well. Figure 10, right, is an example of sea clutter in the dark: it shows a frame recorded on a night with no moon and in absence of artificial lights. The scene presents many false alarms, which cannot be explained by reflected nor refracted thermal energy. This kind of clutter is explained by differences in thermal emission at the surface caused by waves, which result in areas with different apparent temperatures. Specifically, the energy radiated by a surface is proportional to the sine of the angle between the direction of radiation and the surface (Annex, [6]). For maritime observations, the observer is usually standing a few meters above the sea surface and can see at relatively long ranges (greater than few kilometres). Consequently, the observation angle (equal to the emissivity angle) and the emissivity is small, on average. In the presence of a wave, the upslope side of the wave presents a higher angle of emission and looks warmer on average than the surrounding sea surface, causing a false alarm. Conditions in which waves generate differences in IR measurements is called *emitted clutter*.

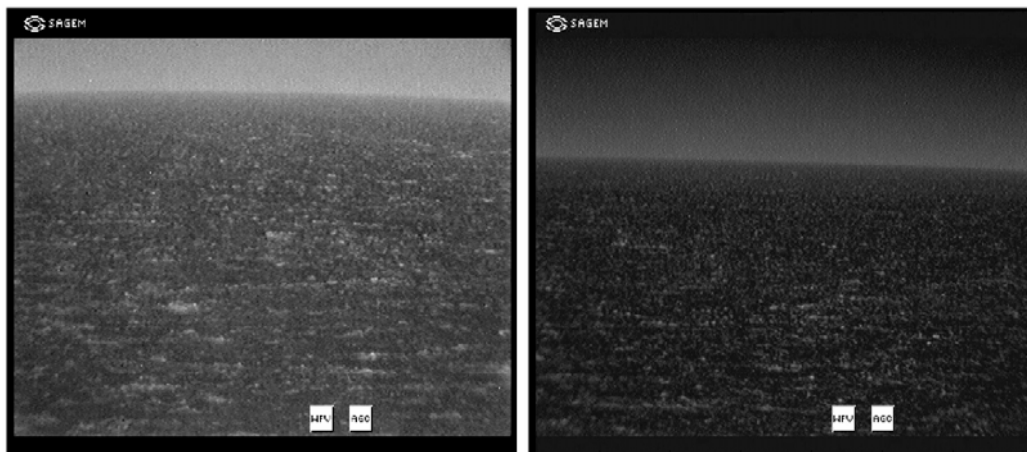


Figure 10 Examples of sea clutter. Left: day time. Right: night time with no moon.

A pictorial representation of the effects of waves on thermal radiation of the sea surface is shown in Figure 11.

In these conditions sightings using IR video are difficult, similar to how visual watch suffers in high sea states and strong winds.

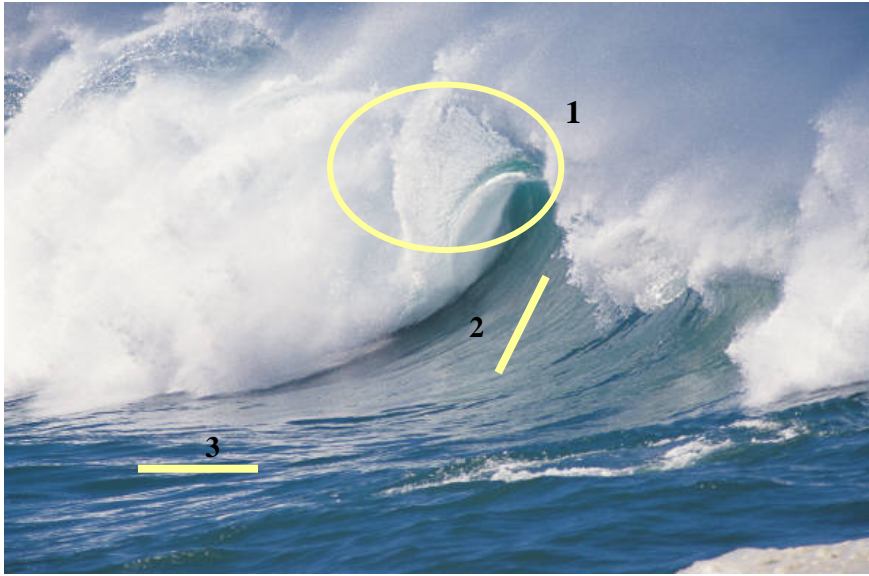


Figure 11 Pictorial representation of wave effects on thermal radiation of the sea surface. 1) Breaking wave: strong clutter. 2) High angle of observation: high emissivity, high apparent temperature. 3) Low angle of observation: low emissivity, low apparent temperature.

5.2 Sensor Calibration and Offline Correction

As shown in the previous section, images in WFV and NFV are very sharp and clear, provided the system has been properly calibrated.

Before starting each acquisition, it is necessary to calibrate the sensor by pointing the IR binocular at a uniform surface (or by putting the black lids over the lenses) and by running the internal calibration test; this test modifies the gain of each detector of the sensor in order to return the most uniform image possible. The result of post-calibration is usually excellent; nonetheless, more calibrations during use may be necessary, especially after long usage periods, or when the field of view is changed from WFOV to NFOV and vice versa.

During the experiment sometimes it was not possible to calibrate the system, because of lack of time. Frames acquired without calibration are affected by saturated pixels (isolated bright pixels) or dark pixels. Offline post-processing, including the use of noise removal filters like the median filter, may improve image quality. The choice of the median filter length (in pixels) is crucial: shorter filters may not effectively remove noisy pixels, while longer filters may blur the image. For this reason, the length of the median filter is chosen on case by case basis depending on the quality of the original image.

An example of poorly calibrated image and the result after offline filtering is shown in Figure 12: this example refers to a cropped image of 350×230 pixels; in this case the median filter length is 5.

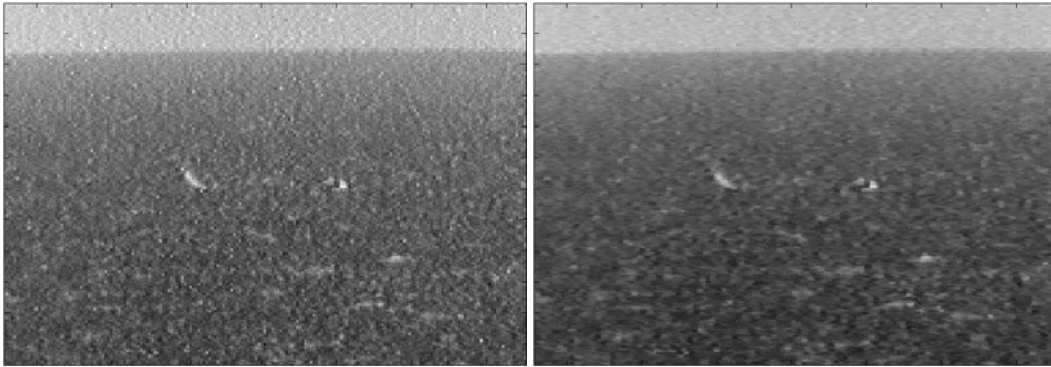


Figure 12 Original uncalibrated frame (left) and corresponding filtered result (right)

5.3 Comparison between Visual Sightings and IR Sightings

Figure 13 is a graphical summary of the visual sightings during Sirena '03 – Phase 1 sea trial. The lines indicate the track of the *Alliance* during the nine days of the experiment (different colours for different days). The marks correspond to the different sightings and are geographically referenced.

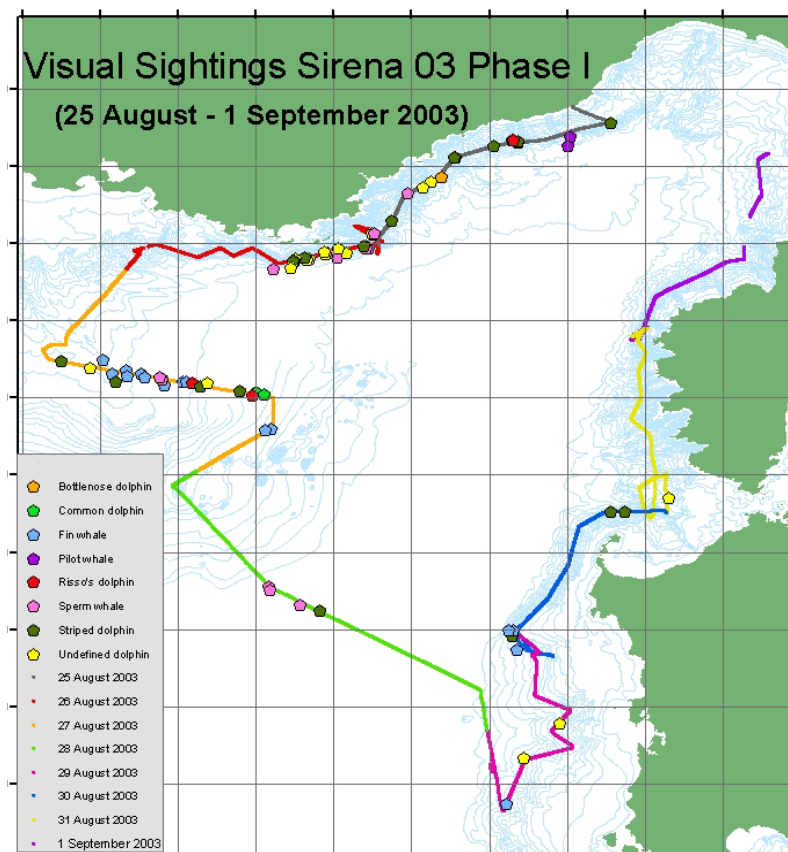


Figure 13 Visual sightings during Sirena '03 – Phase 1.

It is immediately clear that the first three days (25-26-27 August) had the highest number of sightings (18, 19, and 24, respectively). This may have been related to the weather conditions: there was good visibility and low sea state during the first two days; the third day also had a high concentration of animals, even with lower visibility. The weather became much worse during the following days, with strong winds and high sea states. The number of sightings significantly decreased to 4, 3, 6 and 1.

The meteorological data for the first four days (25-28 August) are summarized in Table 2. During the following days sea state values were between 2 and 4.5, and wind speed was always above 10-12 kts, with peaks of 18-20kts.

Table 2 Meteorological data for days 25 – 28 August 2003

	25 August	26 August	27 August	28 August
Air temperature (°C)	26.2÷27.1	24.9÷27.4	26.9÷27.6	27.5÷28.8
Sea temperature (°C)	27.0÷27.8	25.7÷26.8	25.6÷26.7	27.0÷28.5
Humidity (%)	85÷91	91÷83	91÷95	95÷87
Wind speed (kts)	1÷3	2÷15	12÷15	13÷16
Sea State	0.5÷2	2÷4	1÷3.5	3÷4.5
Pressure (hPa)	1008÷1009	1010÷1011	1011÷1012	1009÷1010

Table 3 lists the different species seen during the test and their *species code* used in tables 4-6. Table 4, Table 5, and Table 6 detail visual and IR sightings for 25, 26 and 27 August. The species codes are explained in Table 3. “Aspect” is the animal’s heading relative to the *Alliance* (“6” means animal with course opposite to *Alliance*’s course). In the last column, “Off effort” means that the IR system was off at that sighting time; ✓ means that the animal was sighted with the IR system as well; ✗ means that the animal was not sighted with the IR system; finally, 📹 indicates that the IR video was recorded.







In the following sections the results will be explained for each day separately. As a general rule, visual sightings are used as a reference and the discussion focuses on why there were corresponding IR sightings or not. The IR system was off effort during many visual sightings for one of the following reasons: a) the IR goggles cannot operate indefinitely because battery packs must be replaced after a number of hours; b) it takes around 6 minutes for the IR system to cool, so sometimes the system was cooling during the visual sighting; c) sometimes the system was not pointed in the right direction; d) only one operator was responsible of the IR system and no turn over was available.

Table 3 *Species codes*

Species Code	Species	Italian name	English name
Bp	Balaenoptera physalus	Balenottera comune	Fin whale
Dd	Delphinus delphis	Delfino comune	Common dolphin
Gg	Grampus griseus	Grampo	Risso's dolphin
Gme	Globicephala melas	Globicefalo	Long-finned pilot whale
Pm	Physeter macrocephalus	Capodoglio	Sperm whale
Sc	Stenella coeruleoalba	Stenella striata	Striped dolphin
Tt	Tursiops truncatus	Tursiope	Bottlenose dolphin

5.3.1 25 August 2003

Table 4 *Visual and IR sightings, 25 August 2003*

Sighting #	Time	Species	Aspect	An Course	Range (nmi)	IR sighting
3	8.51	Gme	2	190	1,87	✓ 
5	9.16	Gme	12	157	4,78	✓ 
9	11.03	Sc	5	305	0,61	✓ 
10	11.11	Gg	2	309	1,87	✗
11	11.21	Gg	5	342	1,08	✓ 
17	13.47	Sc	10	253	1,07	✓ 
18	13.56	Sc	12	261	0,48	✓ 

During the first day of observations, NRV *Alliance* followed a track approximately parallel to the Ligurian Coast, corresponding to the 1000m isobath. When the IR system was on duty, all the visual sightings had a corresponding IR sighting, with the exception of sighting #10, probably because of wrong AGC settings. Very high quality video sequences were recorded during this day: see frames in figures 14.16.

It is worth noting that detection of animals is more difficult in single frames than whole video sequences. The movement of the animal is, in fact, tracked by the operator's eye, improving detection performance.



Figure 14 Group of slowly moving striped dolphins (Table 4, sighting #18).

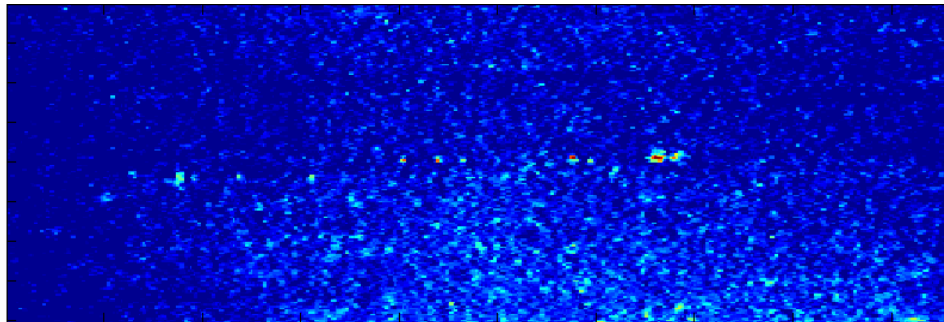


Figure 15 Group of slowly moving striped dolphins - particular with false colours (Table 4, sighting #18).

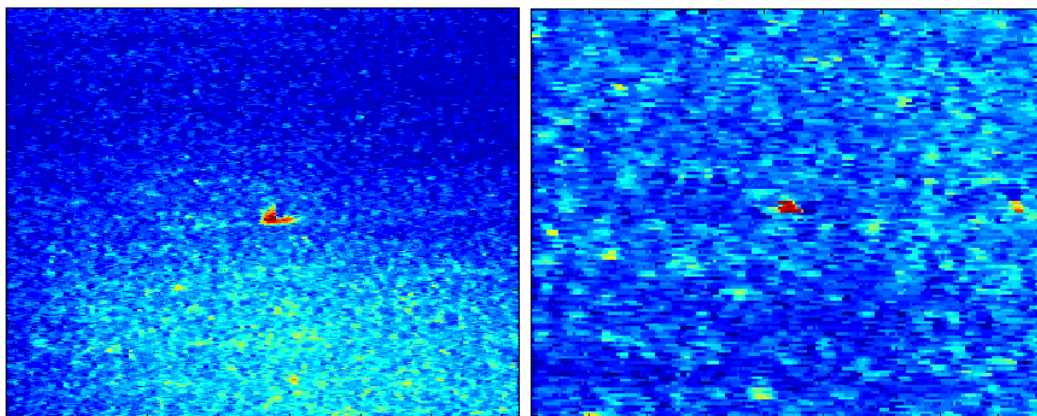






Figure 16 Left: Striped Dolphin jumping (Table 4, sighting #9). Right: Fin of a Striped Dolphin (Table 4, sighting #9).

5.3.2 26 August 2003

Table 5 Visual and IR sightings, 26 August 2003

Sighting #	Time	Species	Aspect	An Course	Range (nmi)	IR sighting
2	9.04	Pm	8	192	1,29	✓ 
4	9.10	Pm		189	1,11	✓ 
9	9.55	Pm		225	4,78	✓ 
11	10.07	UD	7	173	1,29	✓
12	10.14	UD	8	307	1,62	✓
17	10.42	Pm		252	1,62	✓
18	10.44	UD		257	1,87	✓
21	10.56	UD	12	313	1,17	✓
26	11.39	UD	4	217	1,29	✓
29	11.54	UD	12	135	0,30	✓
30	11.56	UD		158	0,76	✓
31	12.01	Sc	7	344	0,39	✓ 

The *Alliance*'s track during the second day was still parallel to the coast (along France), following the 1000m bathymetry profile.

Favourable weather conditions allowed the IR system to detect Sperm Whales sighted during the on effort period. The blow of sperm whales was clearly detected, even at long ranges (more than 4,5 nmi). The fluke and the skin were visible also, probably because the surfacing body offers higher observation angles and, accordingly, higher apparent temperature. Further, the water perturbation due to the motion of the body could be clearly detected. On the other hand, the blow hole was not visible during long-range Sperm Whale sightings.

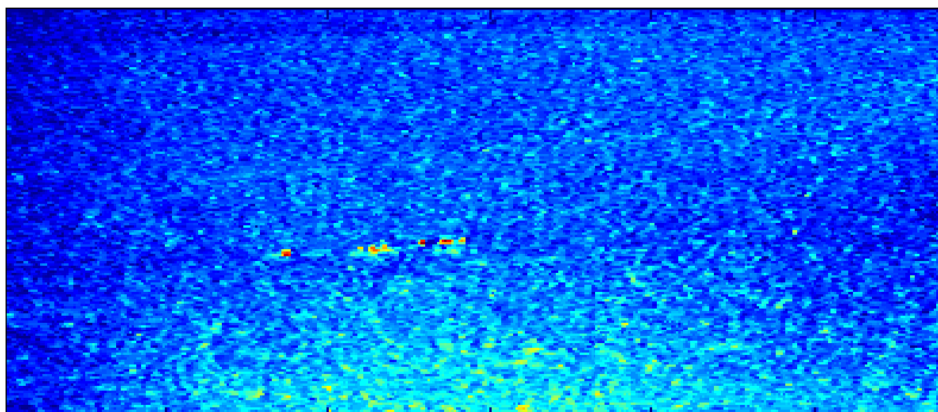


Figure 17 Group of slowly moving striped dolphins (Table 5, sighting #31).

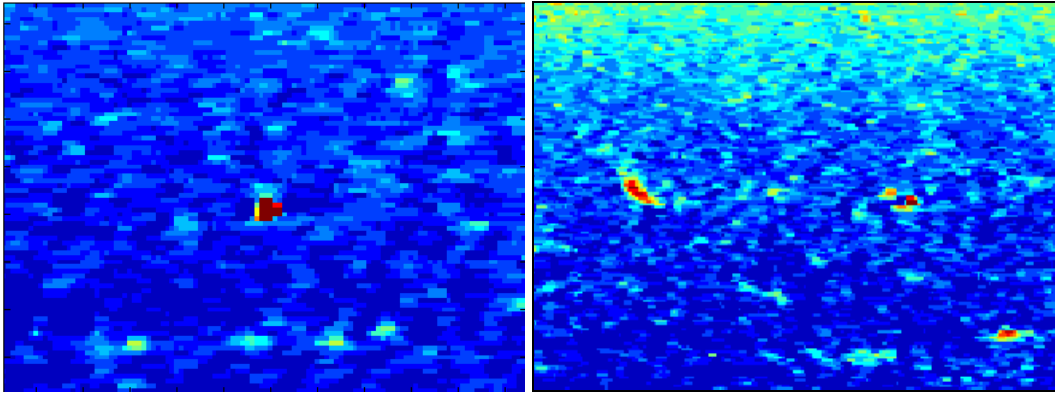


Figure 18 *Left: Back of a diving Sperm Whale. Right: Sperm Whale's blow - particular (Table 5, sighting #4).*

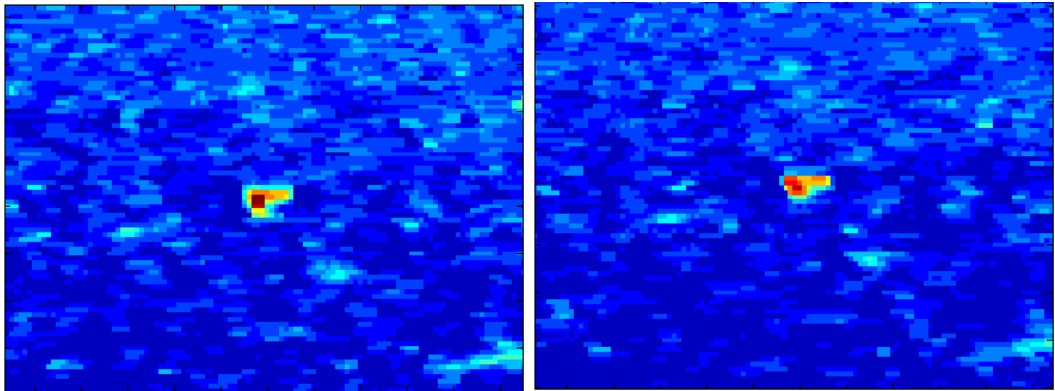


Figure 19 *"Fluke up" of a Sperm Whale.*

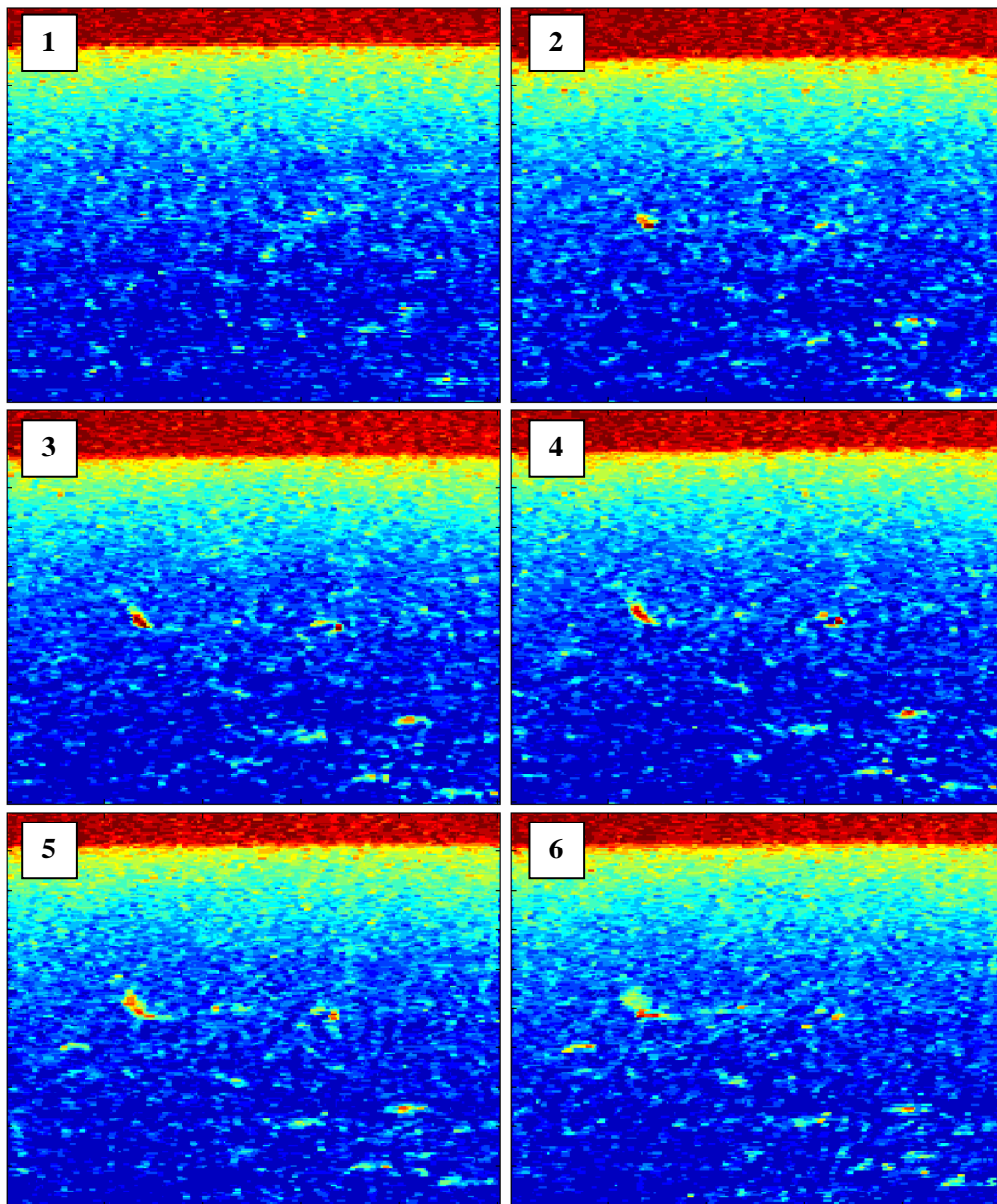


Figure 20 *Sequence of frames showing a Sperm Whale's blow (Table 5, sighting #4).*

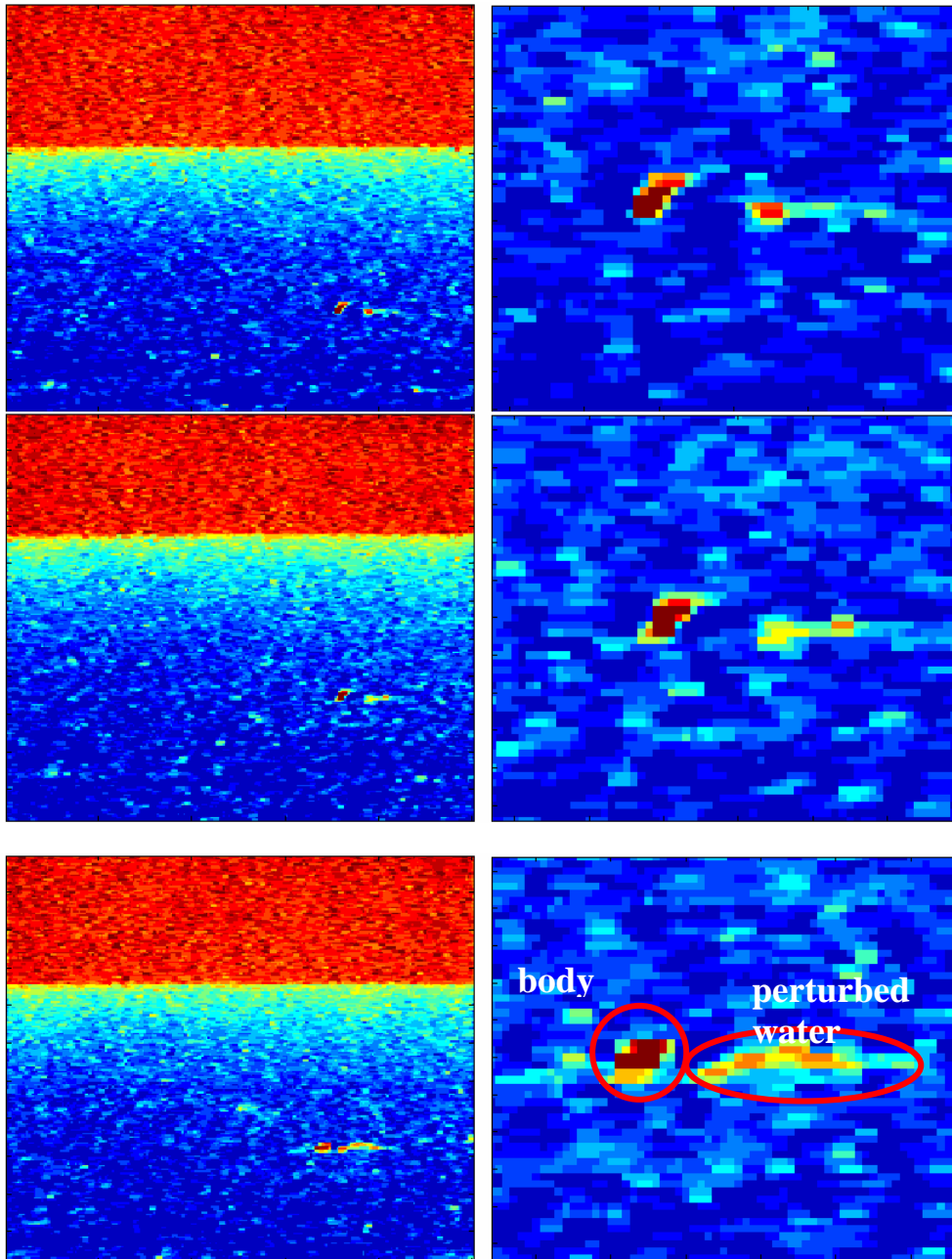



Figure 21 *Sequence of frames showing a diving Sperm Whale (Table 5, sighting #4).*

5.3.3 27 August 2003

Table 6 Visual and IR sightings, 27 August 2003

Sighting #	Time	Species	Aspect	An Course	Range (nmi)	IR sighting
10	9.18	Bp		26	3,64	×
11	9.53	Bp		155	1,35	×
12	10.07	Bp	10	84	3,02	×
13	10.16	Sc		192	3,93	×
14	10.32	Bp	4	141	1,44	×
17	11.03	Bp	11	80	1,87	×
18	11.35	Bp	7	238	0,32	×
19	11.55	Bp	11	97	2,73	×
20	12.09	Bp	10	146	3,40	× 

The third day was characterized by extremely high humidity: the optic of the IR system was covered by condensed water vapour and the digital video camera could not operate because of an internal protection block which prevents damages in case of high humidity. The horizon was not visible. As expected, IR performance degraded dramatically: no detections occurred even in presence of many visual sightings.

5.3.4 28 – 31 August 2003

A total amount of 14 sightings were collected during the last four days of the cruise. This low number was probably due to bad weather conditions, with strong winds and high sea states. The IR system was used for only small periods during these days, because of the strong clutter.

5.3.5 Night time Operations

The IR binoculars were tested during three nights, for a total of about ten hours.

During one of the nights, the acoustic team detected the presence of striped dolphins at a relative short range, but azimuth information was not available. At the time of the acoustic identification, the IR system was on duty, scanning a horizon of about 180 degrees. There were no sightings, however, probably because the IR sensor was pointing the wrong direction. This limitation is common to all narrow FOV systems (even in the visible). In order to fully exploit the advantage of IR technology, either multiple IR cameras pointing different directions or a continuous scanning system are needed.

Nevertheless, IR systems are capable of seeing at night and remain one of the only potential night time mitigation systems, in addition to radar and acoustics.

Lessons Learned and Future Work

This experiment was developed to investigate the feasibility of using the InfraRed technology as an aid to currently adopted mitigation systems, like visual, acoustics and radar.

This experiment showed how performance is strongly affected by weather conditions. IR systems are practically useless with rain, fog or haze, because the water and/or the water vapour in the atmosphere strongly attenuates the thermal radiation and is, as a result, opaque in the IR portion of the electro-magnetic spectrum.

As the relative humidity in the air decreases, IR systems are capable of detecting:

- the blow of big cetaceans (like sperm whales and fin whales), as a mass of particles with temperature higher than the surrounding air;
- changes in emissivity of the water perturbed by the presence of an animal;
- changes in emissivity of the skin of the animal because of its movement (aspect changes).

As for visual systems, white caps are a problem for IR systems, since they generate clutter in IR imagery as well. As a consequence, IR system performance drops quickly as the sea state increases (IR was ineffective with sea state greater than two/three).

Another problem experienced is the long start-up time of the system. In realistic scenarios, IR system should operate continuously; long operations would then reduce the life of the cooling system, which is designed to work for a limited number of hours (of the order of few thousands). This could be a serious limitation for Stirling-cooled devices like the one tested in this experiment.

It was difficult to test the system during the night. As for all narrow field of view systems, performance is limited by the reduced capability of efficiently scanning the horizon.

Possible solutions are:

- use of multiple systems pointing at different directions;
- use of a scanning system, like a platform moving either continuously or step-wise;

- having a cuing system (either radar detections or acoustic detections after some sort of beamforming to estimate the direction of arrival).

During the next experiment, the IR system will be tested mainly at night. Hopefully more than one IR camera will be available on loan, allowing for more detection opportunities, even if not cued by other systems. Should a radar-based whale detection system be available, the radar detections will be used to point the IR system.

The development of a scanning system would still be premature and would be considered only if the effectiveness of IR at night time is demonstrated.

Another important area of investigation is the development of image processing algorithms for image denoising, image enhancement and automatic target detection.

7

Conclusions

IR binoculars were tested during the Sirena'03 – Phase 1 experiment (25 August – 2 September 2003). The aim of this test was to investigate the potential of IR technology for marine mammal detection and identification. Promising results were obtained in daylight when the weather conditions were favourable. In these cases, all of the visual sightings had a corresponding IR sighting. The scenes recorded by the IR system showed the relative differences in thermal emissivity of the sea, due to radiation from the animals' bodies and perturbation of the water by the animals.

The IR system was ineffective in the presence of high humidity, because water vapour strongly attenuated the available thermal radiation. It was not possible to fully test the IR system during the night due to lack of opportunities. During Sirena 06 planned for July and August of 2006, we hope to attempt to track a tagged animal during a "focal follow" experiment. The tag normally has a radio beacon giving the relative position of the animal, which could be used to cue the infrared system.

References

- [1] Di Natale, A., personal communication.
- [2] NURC Instruction No. 77-01, La Spezia, Italy, NATO SACLANT Undersea Research Centre, 2001.
- [3] Baldacci A., Target Detection in IR Video Sequences, PhD Thesis, October 2000.
- [4] Kruer M.R., Scribner D.A., Killiany J.M., IR focal plane array technology development for Navy applications, *Optical Engineering*, Vol 26, No. 3, March 1987, pp. 182-190.
- [5] Crawford F.J., Electro – Optical Sensors Overview, *IEEE Aerospace and Electronic Systems Magazine*, Vol. 13, n. 10, October 1998, pp. 17-24.
- [6] Campana S.B., *The IR & Electro-Optical Systems Handbook. Vol. 5: Passive Electro-Optical Systems*, SPIE Press, 1993
- [7] Cuyler L.C., Wiulsrød R., Øritsland N.A., Thermal IR Radiation from Free Living Whales, *Marine Mammal Science*, 8(2): 120 – 134, April 1992.
- [8] Irving L., *Arctic life of birds and mammals*, Springer Verlag, Berlin.
- [9] Williams T.M., Noren D., Berry P., Estes, J.A., Allison C., Kirtland J., The Diving Physiology of Bottlenose Dolphins (*Tursiops Truncatus*).- III. Thermoregulation at Depth, *The Journal of Experimental Biology* 202, 2763-2769 (1999).
- [10] Sholander, P.F. and Schevill, W.E., Counter – current vascular heat exchange in the fins of whales, *Journal of Applied. Physiology*, 8, 279-282.
- [11] Prunier D., MATIS and LUTIS handheld thermal imagers, *Proceedings SPIE Vol 3698*, pp. 291-307, *IR Technology and Applications XXV*, July 1999.
- [12] MATIS Handheld Technical Description, November 2001 (Company Confidential).
- [13] MATIS Handheld TI User's Guide, Issue 2, October 2001.
- [14] Baldacci A., Carron M., Fortunato N., *Infrared Detection of Marine Mammals*, NURC DVD, March 2005.

Acknowledgments

The authors would like to thank Mr. Edoardo Testino (Angelo Podestà S.r.L, Genova, Italy) and Dr. Bernard Schmitt (SAGEM, France) for loaning us the IR system used for this experiment; this experiment would not have been possible without their help, and technical advices.

Many thanks to C.F. Marco Scariot, head of the “Reparto Optoelettronica” of the MARITELERADAR Institute of the Italian Navy, who suggested the use of the SAGEM MATIS Handheld as a first investigation system.

Thanks a lot to Piero Lorenzelli, who fixed some last minute technical problems with the video acquisition system. Thanks to Bruno Crocetti, of the Engineering Technology Department, who built the mechanical interface between the tripod and the IR goggles and the video camera. Thanks to the Print Shop of the NURC, who provided the tripod.

Many thanks to the Crew of NRV *Alliance* and to the Scientist involved in Sirena’03 Phase 1, who have shown interest, curiosity and enthusiasm for this part of the experiment and encouraged the first author during the long nights spent without any sightings on the flying bridge of the *Alliance*.

Thanks to Maria Elena Quero who provided the sighting reports and the meteorological data recorded during the effort time, and to the Summer Research Assistant Barbara van Mol who provided the GIS images used in this report.

Finally, the first author would like to thank his wife Anna, from whom this work subtracted a lot of time, since all the post cruise analysis was done at home, mainly at night and during the weekends.



IR picture of *Alliance* Crew and Scientist involved in Sirena ’03 Phase 1 Experiment (August 25th – September 2nd 2003).

Annex A Principles of Thermography

All material objects above absolute zero radiate electromagnetic energy. The maximum value of this radiation per unit wavelength is given by Planck's blackbody radiation law,

$$L_{bb}(\lambda, T) = \left(\frac{2\pi^5 hc^2}{15 \lambda^5} \right) \left[\exp\left(\frac{hc}{\lambda kT} \right) - 1 \right]^{-1} \quad (1)$$

where

- c = speed of light in vacuum = 2.997×10^8 ms⁻¹
- h = Planck's constant = 6.626×10^{-34} Js
- k = Boltzmann's constant = 1.381×10^{-23} JK⁻¹
- T = absolute temperature in kelvins
- λ = radiation wavelength in meters.

The radiation of a real object is obtained by multiplying the blackbody radiation term by the spectral emissivity of the object $\varepsilon(\lambda)$:

$$L(\lambda, T) = \varepsilon(\lambda, T) L_{bb}(\lambda, T) \quad (2)$$

Equation (2) can be considered a definition of emissivity.

The total power radiated is given by the integration of equation (1) over all wavelengths, yielding

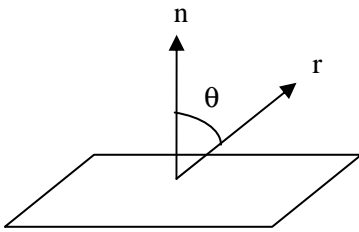
$$L_{bb}(T) = \sigma T^4 \quad (3)$$

where σ = Stefan-Boltzmann constant = 5.67×10^{-8} Wm⁻²K⁻⁴. The rate of change with temperature of a thermal source is therefore

$$\frac{\partial L_{bb}}{\partial T} = 4\sigma T^3 \quad (4)$$

When we measure the radiation emanating from an IR scene, we find variations from point to point due to variations in temperature and emissivity. It is only this variation in radiance that is useful in image formation. The basic concept of a modern FLIR is to form a real image of the IR scene, detect the variation in the imaged radiation, and, by suitable electronic processing, create a visible representation of this radiation.

For an emitting surface, such as the sea surface or the skin of an animal, the radiance is the power emitted, in a given direction and per unit solid angle, by the emitting surface projected on the plane orthogonal to the emitting direction.



FigureA1 *Geometry of an emitting surface*

The projected surface is related to the actual emitting surface by a cosine law:

$$S_r = \frac{S_n}{\cos \theta} \quad (5)$$

As a consequence, when observing a surface, its apparent temperature decreases with the grazing angle according to this cosine law.

Document Data Sheet

<i>Security Classification</i> RELEASABLE TO THE PUBLIC		<i>Project No.</i> 4F1
<i>Document Serial No.</i> SR-443	<i>Date of Issue</i> February 2006	<i>Total Pages</i> 37 pp.
<i>Author(s)</i> Baldacci, A., Carron, M., Portunato, N.		
<i>Title</i> Infrared detection of marine mammals.		
<i>Abstract</i> <p>An infrared (IR) binocular, designed for in-the-field military applications, was tested using in situ marine mammals during the Mar Ligure Joint Experiment 2003 (MLJX'03) that took place in August-September 2003 onboard the NRV <i>Alliance</i>. The test investigated the potential of IR technology for marine mammal detection, in both day time and night time conditions. The effectiveness of this IR system in detecting marine mammals was strongly affected by weather conditions, ranging from excellent performance during clear and low sea-state conditions to poor performance during hazy conditions or higher sea-states. The IR system was tested during both day and night</p>		
<i>Keywords</i> Marine mammal risk mitigation – cetacean – whale – infrared – IR– detection– blow temperature – surface temperature		
<i>Issuing Organization</i> NATO Undersea Research Centre Viale San Bartolomeo 400, 19138 La Spezia, Italy [From N. America: NATO Undersea Research Centre (New York) APO AE 09613-5000]		Tel: +39 0187 527 361 Fax: +39 0187 527 700 E-mail: library@nurc.nato.int